Isotropic Mapping of T_1, T_2, and M_0 with MP-DESS and Phase-Graph Data Fitting

T. Stoecker[1], K. Vahedipour[1], E. Pracht[1], D. Brenner[1], and N. J. Shah[1,2]

[1]Institute of Neuroscience and Medicine - 4, Forschungszentrum Juelich, Juelich, Germany, [2]Department of Neurology, Faculty of Medicine, JARA, RWTH Aachen University, Aachen, Germany

Introduction: Quantitative MRI (qMRI) of the human brain provides important insights into certain pathologies [1]. Isotropic, high resolution is best achieved with a 3D sequence – i.e. a 2D phase encoded (PE) acquisition – using short TR (<T_2). This leads to biased parameter estimates in qMRI approaches where perfect spoiling is assumed [2], for instance Look-Locker approaches. Thus, it is important to incorporate transverse relaxation into the signal equation, as has been carried out in transient balanced SSFP [3-4], which is however prone to banding artefacts induced by B_0-inhomogeneities. Here, a double echo steady state sequence [5] with magnetization preparation, MP-DESS, is utilized to overcome these limitations. An accurate signal equation for least squares data fitting is provided by the extended phase graph [6]. Along the MP-recovery the DESS images, *S*+ and *S*-, are individually reconstructed. The *S*+ state (the "FID") provides a higher SNR whereas the *S*- state (the "Echo") has a more pronounced T_2 weighting. Together they provide high sensitivity for the parameters under investigation, i.e. M_0, T_1, and T_2.

Methods: In a standard 3D-DESS sequence with rectangular pulses of flip-angle α, every Nth pulse is replaced by a rectangular 180° pulse. The recovery echo train of length N is divided in L segments of size M which encode the same k-space, giving L=N/M different images for *S*+ and *S*-, respectively (Fig.1). The outer MP loop has to be performed N_xN_y/M times, where $\{N_x,N_y\}$ denote the PE matrix size. The signal is modelled with the extended phase graph. Since performing these calculations on a voxel-by-voxel basis for data fitting is far too slow, a parallelised computation matching the sequence parameters is pre-calculated on a suitable grid $\{T_1,T_2,W_{RF}\}$, where W_{RF} denotes a spatial B_1 weighting factor, common for the α-pulse and the 180° pulse. This results in a "signal database", $\{\hat{S}_i^+,\hat{S}_i^-\}, i=1,\dots,L$, showing a smooth dependence on the relaxation times. M_0 is a common scaling factor of the signal levels. The signal database is well-suited for rapid tri-linear interpolation in least-squares cost function minimisation: $CF=\sqrt{\sum_{i=1}^{L}\left(s_i^+-\hat{s}_i^+\right)^2+\left(s_i^- -\hat{s}_i^-\right)^2}$. Consequently, the fitting of ≈10^6 voxels needs less than five minutes on an up-to-date desktop PC. Data were acquired on a Siemens TIM-Trio scanner with a 12-channel head array coil (Siemens, Erlangen). W_{RF} was mapped with the 3D AFI sequence [7] (TR1/TR2=5). Receiver sensitivity was corrected by means of a body-coil FLASH image. MP-DESS echo trains were acquired for an agarose phantom and the fitting result compared to spectroscopic measurements of T_1 and T_2. Finally, an *in vivo* whole brain MP-DESS acquisition was performed and T_1, T_2, and M_0 maps were calculated. The MP-DESS sequence parameters were as follows: matrix size=160×160×120, flip-angle α = 10°, resolution = 1.4 mm (isotropic), TR/TE_{S+}/TE_{S-} = 10/3/7 ms, bandwidth = 270 Hz/Pixel, N/L = 360/9, parallel imaging acceleration = 2, and the acquisition time totalled 15 minutes.

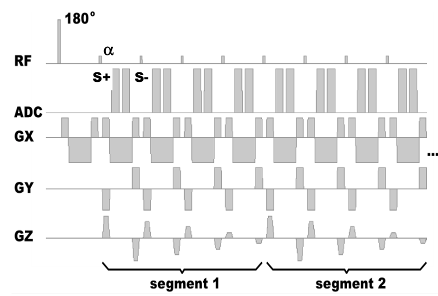

Fig. 1: *MP-DESS Sequence diagram with N=8 and L=2, i.e. M=4 phase encode steps per segment.*

Results: Example slices of the MP-DESS signal database are depicted in Fig. 2a, showing a smooth signal variation with relaxation times. From these the cost function is calculated, shown in Fig. 2b for target parameters T_1/T_2=1000/100 ms. It displays a pronounced global minimum enabling robust parameter estimation in the presence of noise. Fig. 3 compares the echo train measurement and the computed signal amplitudes, showing a nearly perfect match between phantom data and the phase graph signal description. The fitted relaxation-time estimates, T_1/T_2=1683/83 ms, agree with the gold standard spectroscopic evaluation to less than 3% and 8% for T_1 and T_2, respectively. MP-DESS *in vivo* images and parameter mapping results are plotted in Fig. 4. Estimation of cortical relaxation times and the relative spin density agree well with the literature [8].

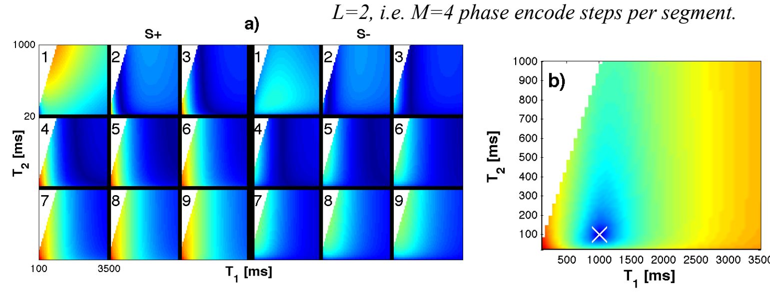

Fig. 2: a) *MP-DESS signal database at* W_{RF} =1 (α=10°, refocusing pulse = 180°). **b)** *Cost function at target* T_1/T_2=1000/100 ms. *Colours denote (arbitrary) units of signal amplitude.*

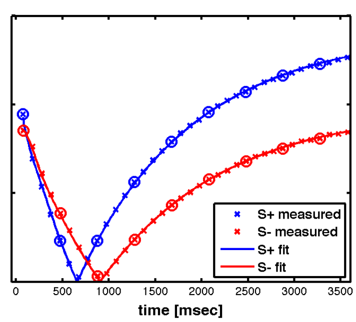

Fig. 3: *Echo train measurements vs. phase graph data fit. The circles mark the nine time-points of the segmented imaging acquisition, at which k-space centerlines were acquired (see Figs. 2 and 3).*

Conclusion: This work presents a novel method for accurate, 3D, high-resolution parameter mapping with time efficient data acquisition, as the MP-DESS sequence and the corresponding phase-graph signal model do not rely on any inter-sequence recovery dead-times. Although the echo train resembles an inversion recovery, the sequence is best understood as generating N different steady states through inversion/refocusing pulses replacing every Nth α-pulse. MP-DESS acquires B_0-insensitive and artefact-free images, as opposed to fully balanced SSFP. Utilising non-selective RF pulses increases the mapping accuracy, as they allow for fast and robust mapping of the B_1 with AFI [7]. The *S*+ and *S*- images provide a robust cost function minimisation which is shown to be most accurate at low flip-angle α. The latter reduces MT effects and supports high field applicability.

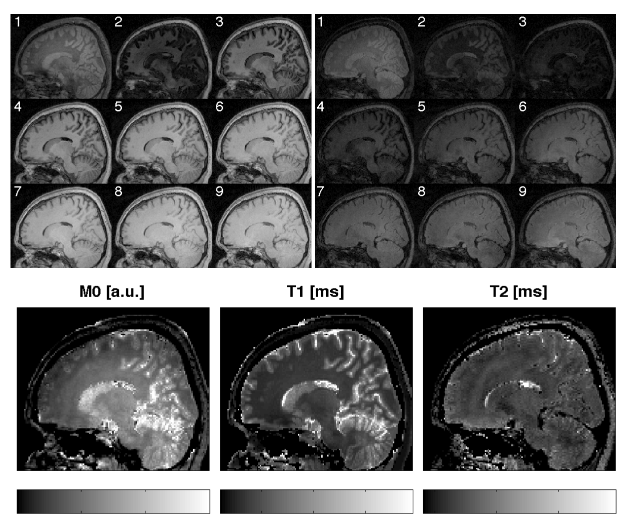

Fig. 4: *Top: MP-DESS images of nine time-points along the recovery curve (left S+; right S-). Bottom: the fitted parameter maps.*

References: [1] Shah et al, NeuroImage 2008:41:706. [2] Neeb et al, NeuroImage 2008:42:1094. [3] Scheffler, MRM 2003:49:781. [4] Schmitt et al, MRM 2004:51:661. [5] Redpath, MRM 1988:2:224. [6] Hennig, Concepts MR 1991:3:125. [7] Nehrke, MRM 2009:61:84. [8] Oros-Peusquens et al, MAGMA. 2008:21:131.